



HHS Public Access

Author manuscript

DNA Repair (Amst). Author manuscript; available in PMC 2019 November 01.

Published in final edited form as:

DNA Repair (Amst). 2018 November ; 71: 33–42. doi:10.1016/j.dnarep.2018.08.005.

MOLECULAR BASIS FOR DAMAGE RECOGNITION AND VERIFICATION BY XPC-RAD23B AND TFIIH IN NUCLEOTIDE EXCISION REPAIR

Hong Mu^a, Nicholas E. Geacintov^b, Suse Broyde^a, Jung-Eun Yeo^c, and Orlando D. Schärer^{c,d,*}

^aDepartment of Biology, New York University, New York, NY 10003 USA

^bDepartment of Chemistry, New York University, New York, NY 10003 USA

^cCenter for Genomic Integrity, Institute for Basic Science, Ulsan, Korea

^dDepartment of Biological Sciences, School of Life Sciences, Ulsan National Institute of Science and Technology, Ulsan, Korea

Abstract

Global genome nucleotide excision repair (GG-NER) is the main pathway for the removal of bulky lesions from DNA and is characterized by an extraordinarily wide substrate specificity. Remarkably, the efficiency of lesion removal varies dramatically and certain lesions escape repair altogether and are therefore associated with high levels of mutagenicity. Central to the multistep mechanism of damage recognition in NER is the sensing of lesion-induced thermodynamic and structural alterations of DNA by the XPC-RAD23B protein and the verification of the damage by the transcription/repair factor TFIIH. Additional factors contribute to the process: UV-DDB, for the recognition of certain UV-induced lesions in particular in the context of chromatin, while the XPA protein is believed to have a role in damage verification and NER complex assembly. Here we consider the molecular mechanisms that determine repair efficiency in GG-NER based on recent structural, computational, biochemical, cellular and single molecule studies of XPC-RAD23B and its yeast ortholog Rad4. We discuss how the actions of XPC-RAD23B are integrated with those of other NER proteins and, based on recent high-resolution structures of TFIIH, present a structural model of how XPC-RAD23B and TFIIH cooperate in damage recognition and verification.

Keywords

DNA Damage Recognition; Nucleotide Excision Repair; XPC-RAD23B; TFIIH; UV-DDB; Molecular Dynamics Simulations

*Corresponding author. orlando.schärer@ibs.re.kr (O.D. Schärer).

Publisher's Disclaimer: This is a PDF file of an unedited manuscript that has been accepted for publication. As a service to our customers we are providing this early version of the manuscript. The manuscript will undergo copyediting, typesetting, and review of the resulting proof before it is published in its final citable form. Please note that during the production process errors may be discovered which could affect the content, and all legal disclaimers that apply to the journal pertain.

Conflicts of Interest

The authors declare no conflict of interest

1. Introduction: Multistep, broad substrate recognition by GG-NER and TC-NER.

Nucleotide excision repair (NER) is a conserved pathway for the repair of a wide variety of bulky DNA lesions that destabilize the DNA duplex [1]. Although the genes involved in prokaryotes and eukaryotes are not conserved, the principles of damage recognition are conceptually similar [2]. NER can occur in two modes. It can be initiated anywhere in the genome by global-genome NER (GG-NER), the main topic of this review, and by a stalled RNA polymerase II in the transcribed strand of active genes by transcription-coupled NER (TC-NER) [3]. Biochemical studies and a number of structures have shown that bulky lesions generally prevent the translocation of RNA polymerase during mRNA synthesis triggering TC-NER, among other responses [4,5].

For efficient recognition in GG-NER, lesions are often substantially larger than normal nucleotides and alter the thermodynamic stability of the local double-stranded DNA structure. Famously, of the two prominent adducts formed by solar UV irradiation, cyclobutane pyrimidine dimers (CPDs) are excised by NER with much slower kinetics than the 6-4 photoproducts (6-4PPs) [6,7], as the latter have a much more destabilizing effect on the DNA duplex [8]. As a consequence, and as shown by recent UV damage-specific whole genome sequencing efforts, CPDs are much more persistent in cells and are therefore thought to be the main cancer-causing lesion generated by UV irradiation [9–11].

Similarly, certain carcinogenic compounds such as the environmental pollutants benzo[a]pyrene (B[a]P) and dibenzo[a,I]pyrene (DB[a,I]P), or the plant-borne mutagen aristolochic acid, can form adducts of different structures that are repaired with dramatically different efficiencies [12]. For example, an N^6 -dA adduct of DB[a,I]P is DNA helix-stabilizing and fully resistant to GG-NER; while an N^2 -dG adduct, with the same stereochemistry at the linkage site to the base as the N^6 -dA adduct, is an excellent substrate [13]. Similarly, an aristolochic acid adduct of dG (N^2 -dG-aristolactam, dG-AL) is readily repaired by NER, while a dA adduct (N^6 -dA-aristolactam, dA-AL) is almost entirely resistant to NER, owing to its unusual and relatively helix stabilizing properties [14,15].

The lack of GG-NER recognition can have very dramatic consequences; dA-AL adducts have been found in cellular DNA samples decades after exposure [16]. As a consequence, A:T → T:A transversion mutations induced by aristolochic acid are associated with upper urothelial cancer. These mutations are exclusively found on the non-transcribed strand of target genes such as p53 and are distinctly recognizable in mutation signatures of tumors [17].

It is well known that the repair efficiency of various NER substrates is generally, although not always, correlated with the degree of thermodynamic destabilization of the DNA double helix caused by a lesion [12,18]. Biochemical and structural studies have further revealed how XPC binding affinity to a given lesion can in many but not all cases explain NER efficiencies [12]. A number of recent reviews, including one in the Cutting Edge in Genome Maintenance series have discussed the mechanisms of damage recognition in NER [3,19–

21]. Here we develop a detailed model of the mechanism of lesion binding by XPC-RAD23B based on recent progress from structural, biophysical, single molecule, computational and biochemical studies and discuss how damage recognition by XPC-RAD23B is integrated with the activities of UV-DDB to recognize lesions, especially CPDs. Finally, we will consider how the handover from XPC to TFIIH takes places, proposing an integrated structural model for damage recognition and verification.

2. The central role of and mechanism used by XPC-RAD23B in damage recognition in NER

2.1. XPC initiates NER for bulky and distorting NER lesions

In *in vitro* reconstituted NER reactions, XPC is necessary and sufficient for the initial damage recognition step [7, 22]. This system, consisting of six core NER factors – XPC-RAD23B, TFIIH, XPA, RPA, XPG and ERCC1-XPF – efficiently repairs large, helix destabilizing lesions (Fig. 1), while it is very inefficient at repairing some non-destabilizing lesions, notably CPDs [6, 23–25]. CPDs are however repaired in cells, albeit with relatively low efficiency, and their repair is dependent on UV-DDB, which facilitates access of XPC in chromatin in cells (see below).

Several lines of evidence have established XPC-RAD23B as the initial damage recognition factor in GG-NER. Competition experiments suggested that XPC-RAD23B binds to lesions before the other core NER factors [22]. Footprinting assays to monitor open DNA formation during NER and sequential binding studies of NER factors to lesion-containing DNA further supported the notion that XPC arrives before TFIIH, XPA, RPA, XPG and ERCC1-XPF [26–28]. Cellular experiments, in which the dynamics of NER proteins was monitored at spatially localized UV damage were consistent with the XPC-first model, as XPC was required for the assembly of all other core NER factors at sites of UV damage [29–31].

2.2. The architecture of the XPC-DNA complex explains its substrate binding preference

The X-ray crystal structure of Rad4, the yeast ortholog of XPC, revealed how the protein binds DNA lesions, using a CPD located in a mismatched sequence as a lesion [32]. It has a sequence- and damage-independent DNA binding domain (TGD/BFID1, yellow and blue, respectively in Fig. 2) that anchors the protein on the DNA and a damage-specific binding domain, made of two β -hairpin modules (BFID2/BFID3, orange and green, respectively in Fig. 2) that interact with the lesion site. XPC might therefore initially bind to DNA non-specifically and use the BHD2/BHD3 domains to search for and sense the presence of DNA lesions. This hypothesis is consistent with the damage-independent association of XPC with chromatin in cells, and a two-stage process to fully engage with lesions [29,33]. The two hairpins of BHD2/BHD3 encircle the *undamaged* strand of DNA (indicated by the two blue Ts in Fig. 2), sensing the single-stranded character induced by the lesion without interacting with the lesion directly [32]. This structure satisfactorily explains the binding preference of XPC-RAD23B and substrate specificity of the overall NER reaction for the majority of lesions [7,34–36].

2.3. Models for XPC recognition from biophysical studies

The question thus arises how XPC-RAD23B finds damaged sites once it has engaged with DNA in the non-specific DNA binding mode. A first clue as to how this may happen came from a structure of Rad4 bound to DNA that did not contain damage [37], made possible by crosslinking the protein to non-damaged DNA through a disulfide crosslink which immobilized the protein bound to DNA in a limited register. Surprisingly, the structure of Rad4 bound to non-damaged DNA was almost indistinguishable from the one with the CPD in a mismatch. A possible answer for how Rad4 may differentiate between lesioned and undamaged sites was obtained using fluorescence spectroscopy experiments measuring the dynamics of opening and closing of a DNA duplex after equilibrium perturbation. These studies showed that the time required for Rad4-induced DNA opening of a 3-base pair mismatched DNA sequence (mimicking lesion-containing DNA) is around 7 ms, which is expected to be much shorter than that for duplex DNA with normal Watson-Crick base-pairing. These studies led to the proposal of the “kinetic gating model”, which suggests that lesion recognition by Rad4 is a result of competition between the residence time of the protein at the lesion site and the time required to form the ‘open’ recognition complex; in damaged DNA the protein resides at the lesion site long enough to form the ‘open’ complex (Fig. 3, biophysical time scale), while this is not the case in undamaged DNA.

More detailed analysis of the Rad4 reaction trajectory using T-jump spectroscopy with fluorescent probes refined this model and revealed a two-step recognition process, termed ‘twist-opening’; it consists of a fast initial “untwisting” step, likely constituting a first test for the deformability of the DNA duplex; this is followed by the slower helix opening and hairpin insertion step [38]. Consistent with this interpretation, BHD3 deletion mutants can mediate the twisting motion but not the full opening, showing that BHD3 is dispensable for the twisting step and lending further support to the two-step model.

2.4. The existence of initial encounter complexes is supported by single molecule studies

The encounter of Rad4 with DNA lesions was further studied in single-molecule studies containing UV-induced CPD lesions strung along DNA duplex “tightropes” [39]. This work demonstrated that Rad4-Rad23 interacts with UV-damaged DNA in three ways. A fraction of Rad4 in this model system is immobilized on the DNA, suggesting tight lesion binding; a second fraction moves randomly along the DNA, representing an unbound fraction; and at first glance unexpectedly, a third fraction displays a constrained motion within 1000 - 2000 base pairs of the lesion. Intriguingly, this constrained motion state can be achieved with Rad4 lacking the BHD3 domain and may therefore be related to the untwisting step delineated from structural data and T-jump experiments (Fig. 3, single molecule). It has been proposed that this constrained motion may be akin to a first responder state that surveys and marks the damaged region, before proceeding to the proper full binding mode. Intriguingly, loss of the tip of the BHD3 domain (a crucial element of the interaction of Rad4/XPC with lesion sites, does not affect overall NER activity or cellular UV survival. Additionally, AFM experiments showed that Rad4 lacking the BHD3 entirely can still bend DNA, suggesting that lesion recognition by Rad4/XPC is a multifaceted process and that perhaps the constrained motion mode can be a highly dynamic mode of homing in on a lesion. A key structural question is how Rad4 can move along the helix by a one-dimensional diffusion

mechanism and to what extent this involves twisting and bending. It is worth noting that this diffusive motion is most likely bi-directional. Earlier biochemical studies have shown that XPC-RAD23B can bind to a mismatch in the absence of a lesion, and together with TFIIH and XPA translocate along the DNA duplex for up to ~ 1000 base pairs in order to locate a little-distorting CPD residue [40]. This observation is consistent with the “first responder” concept and it will be interesting to see how addition of TFIIH and XPA would change the motion of Rad4/XPC on DNA in single molecule experiments [40, 41]. It is furthermore possible that the fraction of the protein with constrained motion would be significantly lower with lesions that bind Rad4/XPC more avidly than CPDs or fluorescein-modified thymine (Fl-dT), a hypothesis that could readily be addressed in future single molecule studies.

2.5. Computational modeling of XPC-RAD23B recognition trajectories

While these biophysical studies have yielded profound insights into the dynamics of the interaction of Rad4/XPC with duplexes containing various degrees of destabilization, they have not yet revealed how Rad4/XPC binds to a physiologically relevant lesion, as they were all carried out with artificial substrates. The question therefore arises if there are additional, lesion-dependent binding modes of XPC. This void is beginning to be filled by computational studies using molecular dynamics simulations with free energy calculations. In these efforts, the trajectories and energetics of Rad4 engaging with different lesions is explored. A first study determined the pathway for Rad4 binding to a CPD lesion in a 3-base pair mismatch [42], identical to the DNA used in the original Rad4 crystal structure [32]. The most energetically favorable trajectory consisted of an initial encounter of the BHD2 hairpin with the nucleotides opposite the lesion in the minor groove (Fig. 3, computed binding pathway, CPD). This results in some initial DNA distortion with low free energy for this intermediate state (~0.8 kcal/mol). The subsequent steps are the full flipping and encircling of the two T bases opposite the lesion in a correlated motion to the transition state, followed by the insertion of the BHD3 hairpin from the major groove to achieve the open complex observed in the X-ray structure [32]. The transition state energy of this pathway is ~4.2 kcal/mol and thus represents the rate limiting step of Rad4 lesion binding. Importantly, the binding free energy profile and the structures along the pathway provide molecular explanations for several previous experimental observations, such as the energy profile derived from the T-jump studies [37, 38] and the observation that the BHD3 domain was not required for an initial encounter with UV-damaged sites in cells or single molecule studies [33, 39]. The study also highlights the importance of the aromatic residues on BHD3 for full damage recognition (Fig. 3) [32].

Subsequent molecular dynamics / free energy studies explored the binding of Rad4 with a B[a]P-derived DNA lesion [43]. The polycyclic aromatic B[a]P is one of the most important environmental pollutants; metabolic activation produces diol epoxide intermediates that react with the exocyclic amine groups of dA and dG, yielding several stereoisomeric covalent DNA adducts. These adducts assume different three-dimensional conformations that depend on their stereochemistry [44] as well as sequence context [45, 46]. These parameters greatly influence their rates of excision by NER mechanisms [13, 35, 47]. The computational studies focused on a *cis*-B[a]P-dG adduct of which the NMR solution structure is known [48], which is an excellent substrate of NER [43]. In the NMR structure

the cytosine opposite the *cis*-B[a]P-dG is extruded from the helix into the major groove. The simulations showed the cytosine to be the first point of encounter with Rad4 – in this case with the BHD3 domain; specifically Phe599 on the tip of the BHD3 hairpin engages with the orphaned base by stacking early on (conformational capture of the extruded partner C, Fig. 3, Initial Binding). This leads to BHD2 and BHD3 further probing and distorting the duplex, rupturing the base pair adjacent to the lesion and displacing the B[a]P ring system toward the minor groove, coupled with the BHD3 hairpin becoming poised for insertion from the major groove (Fig. 3, Transition State). Subsequently, the cytosine base opposite the lesion and its 3' neighbor become fully encircled by their binding pockets in BHD2 and BHD3, the B[a]P residue fully extrudes into the minor groove while the BHD3 hairpin becomes fully inserted and the Phe599 on its tip is stacked with an adjacent base pair (Fig. 3, Productive Binding State). This binding path differs significantly from the one deduced for the small CPD lesion opposite mismatched thymines, where the partner bases are not initially extruded and captured. These two studies illustrate how lesion-binding by Rad4/XPC can be achieved by different pathways to initiate NER.

2.6. Predicting NER susceptibility from initial encounter complexes

Since lesion recognition by Rad4/XPC is necessary for the subsequent cascade of events in GG-NER, we sought to explore how the initial binding of XPC might be influenced by the conformations of bulky B[a]P-dG adducts in DNA. The objectives of such studies are to elucidate the reasons why there is such a variation in the repair rates of different DNA adducts [12]. Molecular dynamics simulations of initial encounter complexes of Rad4/XPC with lesion-containing duplexes were conducted to obtain initial binding trajectories and structures. The results revealed a dependence of Rad4/XPC binding on the conformations of the lesions in the initial stages (Mu, Geacintov, Zhang, and Broyde, unpublished). The following are examples of interdependent parameters investigated to characterize the initial binding of XPC to the lesions and show promise as gauges of experimentally observed NER resistance: (1) conformational capture of the partner base on the strand opposite the lesion; (2) the occupied alpha space (AS) volume; this volume reflects the curvature and surface area of the minor groove that is occupied by BHD2 ; (3) untwist angle of the DNA around the lesion site. These are illustrated here with examples of three B[a]P adducts.

In the case of the high NER efficiency (+) *cis*-B[a]P-dG:dC adduct (Fig. 4A, Movie S1), the partner dC is initially extruded from the helix into the major groove by the intercalated B[a]P polycyclic aromatic ring system, and is readily captured by the aromatic residues on the tip of the BHD3 (especially F599). The binding of BHD2 is further stabilized by the interaction of arginine R494 with the backbone of the orphaned C, with concomitant establishment of a large occupied AS volume in the minor groove, leading to local DNA untwisting of about 32°.

In the case of the minor groove (+) *trans*-B[a]P-dG:dC adduct (G*), the G*:C base pair is intact and the B[a]P residue is located in the minor groove (Fig. 4B). Consequently, the initial interaction between BHD2 and the minor groove and the untwisting are less pronounced. Furthermore, the intact base pair hinders the engagement of the aromatic tip of

BHD3 with the base opposite the lesion. These factors are consistent with the lower NER activity of this lesion compared to the corresponding (+)-*cis* adduct.

An example of an NER-resistant adduct is the (+) *cis*-B[*a*]P-dG lesion in the context of a deletion duplex (G*:Del), that is lacking a partner nucleotide opposite G*. The G*:Del duplex is not bound by XPC (K. Feher, N.E. Geacintov, to be published) and it is fully resistant to NER [35, 49]. The bulky B[*a*]P residue in the G*:Del duplex is intercalated between adjacent base pairs; the multiple aromatic rings of the B[*a*]P that replace the position of the absent partner C more than compensate energetically for the deleted dC [2, 49]. Due to the thermodynamic stability of the G*:Del duplex and the lack of the nucleotide opposite the lesion, neither the BHD3 nor the BHD2 hairpin can engage with the lesion site (Fig. 4C, Movie S2). As a consequence, the BHD2 domain establishes more limited contact with the lesion site than even the (+)-*trans*-B[*a*]P-dG* adduct and fails to untwist the G*:Del duplex to initiate NER.

These examples show that molecular modeling/dynamics of initial encounter complexes, with determination of the occupied AS volume by BHD2 in the DNA minor groove and untwist angles provide structural hallmarks of initial XPC binding. These characteristics explain the lack of XPC binding with consequent absence of NER activity, here exemplified by the (+)-*cis*-G*:Del duplex, and show potential in estimating NER resistance of DNA adducts with known conformations. Hence weak initial binding is a first indicator of poor NER activity; this has been shown in a study of a series of 12 adducts whose NER activities vary from resistant to highly efficient (Mu, Geacintov, Zhang, and Broyde, to be published).

XPC binding affinity is correlated with NER efficiencies in human cell extracts for many DNA lesions [7, 15, 50, 51], but not for B[*a*]P in certain base sequence contexts or for certain other polycyclic aromatic DNA adducts [52]. Indeed, experiments using such model substrates suggest that XPC can also form non-productive complexes with DNA adducts that do not lead to proper NER preincision complex assembly and formation of dual incision products. The molecular modeling studies are providing structural insights into how the differences in the recognition by Rad4 of structurally diverse DNA lesions result in variable levels of repair susceptibility [42, 43]. The availability of sets of DNA lesions with known structural features and characterization of relative NER efficiencies in human cell extracts [12] provides a fertile experimental basis for further elaboration of the structure-function relationship in lesion recognition and NER resistance by computational approaches.

3. Handover from UV-DDB to XPC and from XPC to TFIIH

While XPC-RAD23B clearly occupies a central role in damage recognition and the initiation of the multi-step NER mechanism, factors acting upstream and downstream of this binding step are important for damage recognition and verification. Much progress has been made in elucidating how UV-DDB recognizes CPD lesions in chromatin, the handover from UV-DDB to XPC-RAD23B, and the damage verification step by TFIIH. These aspects of NER have been the subject of several recent reviews [19–21, 53, 54]. We will therefore focus our discussion here on the interplay of these factors with XPC-RAD23B and present a structural

model for how XPC-RAD23B and TFIIH work together to recognize and verify DNA lesions.

3.1. UV-DDB: Delivering non-distorting and chromatinized DNA lesions to XPC

The mechanism of damage-recognition by XPC/Rad4, described in section 2, does not explain how the minimally distorting CPD UV lesion is repaired by NER. It also does not explain how NER occurs in the context of chromatin. The UV-damaged DNA binding protein (UV-DDB, consisting of DDB1 and DDB2/XPE) is central to both of these aspects of NER (Fig. 1). UV-DDB has a higher affinity for DNA lesions than XPC-RAD23B, especially for CPD [55–57]. Structural studies have shown that DDB2 inserts itself as a wedge into the duplex at the lesion site, flipping out the two nucleotides of the CPD into a shallow binding pocket, which can accommodate lesions such as CPDs, 6-4PPs, or abasic sites by shape complementarity [58–60]. In contrast to XPC, DDB2 therefore directly interacts with lesions. It induces a kink into the duplex that may facilitate the subsequent handover to XPC. Simple overlay of the structures of XPC/Rad4 and DDB2 bound to DNA suggests that the two proteins cannot bind DNA lesions simultaneously. Furthermore, adding UV-DDB to an *in vitro* reconstituted NER reaction does not appear to dramatically increase the repair of CPDs [6], suggesting that a more complex handover mechanism is at work.

In cells, DDB2 is clearly required for the recruitment of XPC and the repair of CPDs [61, 62]. The complexity of the roles of UV-DDB2 became apparent when it was found that DDB1 serves as a connector protein for the ubiquitin ligase CUL4-RBX1 [63]. The UV-DDB2-CUL4-RBX1 complex ubiquitinates a number of proteins in response to UV damage, including UV-DDB itself, XPC and histones via Lys48-linked ubiquitin chains [64], initiating a number of regulatory cascades of NER. The ubiquitination of DDB2 leads to its proteasomal degradation after extraction from NER complexes by the segregase VCP/p97 [64,65]. Ubiquitination of XPC by contrast increases its DNA binding activity [64]. XPC is however sumoylated and ubiquitinated for a second time, now via K48 ubiquitin chains by RNF111 [66,67]. These modifications have been shown to be important for the handover of DDB2 to XPC and also for the release of XPC from damaged sites, which is required for progression through the NER pathway.

The activities of XPC-RAD23B and NER more generally are also profoundly influenced by proteins that alter the chromatin state, including chromatin remodelers or histone modifying enzymes, consistent with the access-repair-restore model originally proposed for the repair of DNA lesions in chromatin 40 years ago [68]. Details of how such enzymes influence XPC-RAD23B and NER activity have been reviewed elsewhere and is not our focus [69, 70]. New facets of regulation of NER in chromatin continue to be discovered: recent findings include chromatin modifiers that facilitate the UV-DDB2 to XPC and the XPC to TFIIH handovers as well as the direct interaction of XPC with histone variants [71–73]. The discovery that polyribosylation by PARP1 of DDB2, XPC and chromatin remodelers in an CUL4A-RBX1-independent fashion contribute to damage recognition in chromatin further add to the complexity of the NER reaction in a chromatin environment and certainly stimulate further investigations [74–78].

3.2. Handover from XPC to TFIIH: transitioning from damage recognition to damage verification

Since the propensity to bind to a destabilized duplex without a lesion allows XPC-RAD23B to interact with DNA that is simply destabilized by base pair mismatches, NER employs a second damage verification step that ensures the presence of a lesion. All the available evidence points to a key role for TFIIH in this process. TFIIH is a ten-subunit complex consisting of the core (XPB, XPD, p62, p52, p44, p34 and p8) and CAK (CDK7, cyclin H and MAT1) subunits [79]. While the CAK subunit dissociates from TFIIH during NER [80], core TFIIH remains bound to the lesion-containing fragment until after excision and it is found associated with the excised damage-containing oligonucleotide [81, 82].

Of critical importance for NER are the activities of the two helicase subunits of TFIIH, XPB and XPD. Current models suggest that the role of XPB may be to pry open the DNA to allow the loading of TFIIH and specifically XPD to DNA [83, 84]. Therefore, its role in NER is not as a processive helicase. XPD by contrast is an active 5'->3' helicase in NER and key to the damage verification process [85, 86]. Structural and functional studies of XPD suggest that it tracks along DNA while pulling the DNA through a narrow tunnel that would be too small for bulky DNA lesions to pass through [87-92]. This observation provides a remarkably easy mechanism for damage verification, simply based on size. It has been known for a long time that the helicase activity of the yeast homolog of XPD, Rad3, is blocked by DNA lesions [93]. Similarly, it has been shown that the translocation of archaeal XPD homologs can be blocked by bulky lesions, although the molecular details of XPD stalling at lesions are not yet fully understood [94-96].

Intriguingly, TFIIH has the ability to locate and stall at a lesion from a distance, for example when XPC-RAD23B is loaded onto a mismatch and is allowed to track along the DNA until it encounters a CPD lesion a few hundred nucleotides away [40]. It will be intriguing to determine if TFIIH would be able to similarly add directionality to the constrained motion mode of XPC-RAD23B in single molecule experiments [39]. The XPA protein has also been shown to be present in a ternary complex in the lesion scanning mode. XPA has furthermore been shown to stimulate the overall helicase activity of TFIIH, while at the same time inhibiting the helicase activity in the presence of lesions [41]. It is therefore likely that XPA also contributes to damage verification. This is consistent with its ability to bind kinked DNA structures, which may reflect NER reaction intermediates, in which bubble-like structures are beginning to form [97,98].

3.3. A structural model for the interplay of XPC and TFIIH

XPC has two known interaction sites with TFIIH. It interacts via its N-terminus with the pleckstrin homology (PH) domain of the p62 subunit [99, 100] and the C-terminus of XPC with the XPB subunit [101-103] and both interactions are needed for full NER activity. The interaction between p62 and XPC has been characterized at the structural level and it has been shown that a C-terminal region of XPC (residues 124-141) binds to the PH domain of p62 [100]. Mutation of conserved residues, such as W133, which occupies a binding pocket on the surface of the PH domain, impacts NER activity.

Recent advancements in Cryo-EM approaches have yielded unprecedented insights into the structure of TFIIH. Two high-resolution structures of TFIIH have been solved, as the ten-subunit complex [104] and as part of a transcription complex [105]. Although not all the parts of TFIIH are resolved to high resolution, both structures show that TFIIH assumes a horseshoe-shaped structure with XPB and XPD positioned at either open end and the remaining core subunits aligning with the arc (Movie S3). Each of the two structures provides information on unique elements. The structure by Greber et al. shows how a long α -helix of the CAK subunit MAT1 links XPB and XPD, suggesting that they assume a rigid conformation in the presence of the CAK subunit [104]. One possible implication is that upon dissociation of the CAK subunit from the core TFIIH during NER [80], the relative position of XPB and XPD becomes more flexible, which may be important during the translocation of XPD toward the lesion. This idea is supported by an overlay with the second TFIIH structure by Schilbach et al. [105], which lacks MAT1. If the two structures are superimposed at the XPB/Ssl2 subunits, the conformational change of TFIIH in the absence of MAT1 becomes apparent (Movie S3). The distance between XPB and XPD at the opening of the horseshoe is much greater in the absence of MAT1 and this increased flexibility is likely critical for the translocation of XPD during the damage verification step. The structure by Schilbach revealed two additional unique features: i) XPB is bound to a DNA duplex, revealing how XPB engages with DNA and ii) clear density maps for larger parts of p62, in particular the PH domain that interacts with XPC and is located adjacent to XPD [105].

These structures together with our knowledge of Rad4/XPC and functional data, have allowed us to construct a model for how XPC and TFI IH interact to transition from the damage recognition to the damage verification step (Fig. 5). After XPC engages with the lesion, its C-terminus is located on the 5' side of the lesion (left in Fig. 5A), where it is able to interact with XPB. We modeled the DNA-bound XPB (green ribbons) from the Schilbach structure [105] adjacent to the C-terminus of XPC/Rad4, which positions the horseshoe of TFIIH such that the subunit located closest to the lesion is XPD (salmon color in Fig. 5). We envision that the flexibility of TFIIH, facilitated by the departure of the CAK subunit and with it the MAT1 helix that connects XPB and XPD (Movie S3) will allow the XPD helicase to load onto the DNA, where it can then track along the DNA in a 5' \rightarrow 3' direction until it engages with the lesion (Fig. 5B). In this position, the PH domain of p62 (blue in Fig. 5) that is on the back side of XPD, is in the vicinity of the N-terminus of XPC (which is lacking from the X-ray structure of Rad4), so that the two can engage in an interaction to stabilize the XPC-TFIIH-DNA complex.

Following engagement of TFIIH with the XPC-lesion complex, damage recognition and verification is accomplished, and the asymmetry of the NER complex is established. The NER pre-incision complex assembly is completed by XPA, which interacts with TFI IH and stabilizes the opened bubble together with the single-stranded binding protein RPA [27, 106]. XPA is also responsible for the engagement of ERCC1-XPF [107], the nuclease making the incision 5' to the lesion [108]. XPG, the second endonuclease making the incision 3' to the lesion arrives at the NER complex by interaction with TFIIH [109, 110] and replaces XPC in the pre-incision complex. The first incision 5' to the lesion by ERCC1-XPF only takes place after the pre-incision complex assembly is completed, followed by

initiation of repair synthesis, 3' incision by XPG, completion of repair synthesis and ligation of the nick to restore the original DNA sequence [111–113].

4. Conclusions and perspectives

The characteristic NER dual incision reaction was discovered and reconstitution of the NER reaction achieved in the 1990s [23, 24]. Since then studies of the repair of many different lesions has revealed that the repair rates vary greatly, depending on the physical size, conformation, base sequence context, and impact on the local B-DNA structure. These properties affect how lesions interact with NER proteins, in particular the damage sensor XPC-RAD23B, resulting in efficient, slow or no repair. Here we reviewed advances in understanding the interaction of XPC and its yeast ortholog Rad4 with DNA lesions, based on biochemical, biophysical, single molecule and computational studies. In particular, recent studies have provided computationally derived binding pathways with Rad4/XPC that offer a tool for gauging the overall NER efficiencies that are experimentally benchmarked.

Furthermore, studies of the earliest encounter of Rad4 with lesion-containing duplexes have indicated promise in predicting NER repair resistance. We furthermore discussed the subsequent step in NER, the verification of the size of the lesion by TFIIH. Drawing from recent cryo-EM structures of TFIIH, we generated a model for how XPC-RAD23B and TFIIH cooperate to detect and verify DNA lesions based on specific protein-DNA and protein-protein interactions. We expect that the coming years will provide further exciting structural and mechanistic insights into how NER is able to achieve the repair of a very wide range of structurally diverse lesions, without incising undamaged DNA.

Supplementary Material

Refer to Web version on PubMed Central for supplementary material.

Acknowledgments

We thank Drs. Bennett van Houten (University of Pittsburgh) and Jung-Hyun Min (University of Illinois at Chicago) for insightful discussions and helpful comments on the manuscript. This work was supported by grants from the Korean Institute for Basic Science (IBS-R022-A1-2017 to ODS), the NCI (P01-CA092584 and R01-CA218315 to ODS, R01-CA75449 to SB), the NIEHS (R01-ES025987 to SB and R01-ES024050 to NEG). We gratefully acknowledge resources provided by the Extreme Science and Engineering Discovery Environment (XSEDE), which is supported by National Science Foundation (NSF) Grant MCB060037 to SB, and the NYU IT High Performance Computing Resources and Services.

Abbreviations:

GG-NER	global genome nucleotide excision repair
TC-NER	transcription coupled nucleotide excision repair
CPDs	cyclo pyrimidine dimers
6-4PPs	4-6 photo products
B[a]P	benzo[a]pyrene
AL	aristolactam

BHD beta hairpin domain

References

- [1]. Gillet LC, Schärer OD, Molecular mechanisms of Mammalian global genome nucleotide excision repair, *Chem. Rev.* 106 (2006) 253–276. [PubMed: 16464005]
- [2]. Liu Y, Reeves D, Kropachev K, Cai Y, Ding S, Kolbanovskiy M, Kolbanovskiy A, Bolton JL, Broyde S, Van Houten B, Geacintov NE, Probing for DNA damage with beta-hairpins: similarities in incision efficiencies of bulky DNA adducts by prokaryotic and human nucleotide excision repair systems in vitro, *DNA Repair* 10 (2011) 684–696. [PubMed: 21741328]
- [3]. Marteijn JA, Lans H, Vermeulen W, Hoeijmakers JH, Understanding nucleotide excision repair and its roles in cancer and ageing, *Nat. Rev. Mol. Cell Biol* 15 (2014) 465–481. [PubMed: 24954209]
- [4]. Nadkarni A, Burns JA, Gandolfi A, Chowdhury MA, Cartularo L, Berens C, Geacintov NE, Scicchitano DA, Nucleotide Excision Repair and Transcription-coupled DNA Repair Abrogate the Impact of DNA Damage on Transcription, *J. Biol. Chem* 291 (2016) 848–861. [PubMed: 26559971]
- [5]. Wang W, Xu J Chong, D. Wang, Structural basis of DNA lesion recognition for eukaryotic transcription-coupled nucleotide excision repair, *DNA Repair*. this issue (2018).
- [6]. Reardon JT, Sancar A, Recognition and repair of the cyclobutane thymine dimer, a major cause of skin cancers, by the human excision nuclease, *Genes Dev.* 17 (2003) 2539–2551. [PubMed: 14522951]
- [7]. Sugasawa K, Okamoto T, Shimizu Y, Masutani C, Iwai S, Hanaoka F, A multistep damage recognition mechanism for global genomic nucleotide excision repair, *Genes Dev.* 15 (2001) 507–521. [PubMed: 11238373]
- [8]. Kim JK, Patel D, Choi BS, Contrasting structural impacts induced by cis-syn cyclobutane dimer and (6-4) adduct in DNA duplex decamers: implication in mutagenesis and repair activity, *Photochem. Photobiol* 62 (1995) 44–50. [PubMed: 7638271]
- [9]. Adar S, Hu J, Lieb JD, Sancar A, Genome-wide kinetics of DNA excision repair in relation to chromatin state and mutagenesis, *Proc. Natl. Acad. Sci. USA* 113 (2016) E2124–2133. [PubMed: 27036006]
- [10]. Hu J, Adebali O, Adar S, Sancar A, Dynamic maps of UV damage formation and repair for the human genome, *Proc. Natl. Acad. Sci. USA* 114 (2017) 6758–6763. [PubMed: 28607063]
- [11]. Mao P, Smerdon MJ, Roberts SA, Wyrick JJ, Chromosomal landscape of UV damage formation and repair at single-nucleotide resolution, *Proc. Natl. Acad. Sci. USA* 113 (2016) 9057–9062. [PubMed: 27457959]
- [12]. Geacintov NE, Broyde S, Repair-Resistant DNA Lesions, *Chem Res. Tox* 30 (2017) 1517–1548.
- [13]. Kropachev K, Kolbanovskiy M, Liu Z, Cai Y, Zhang L, Schwaid AG, Kolbanovskiy A, Ding S, Amin S, Broyde S, Geacintov NE, Adenine-DNA adducts derived from the highly tumorigenic Dibenzo[a,l]pyrene are resistant to nucleotide excision repair while guanine adducts are not, *Chem Res. Tox* 26 (2013) 783–793.
- [14]. Lukin M, Zaliznyak T, Johnson F, de los Santos C, Structure and stability of DNA containing an aristolactam II-dA lesion: implications for the NER recognition of bulky adducts, *Nucleic Acids Res.* 40 (2012) 2759–2770. [PubMed: 22121223]
- [15]. Sidorenko VS, Yeo JE, Bonala RR, Johnson F, Schärer OD, Grollman AP, Lack of recognition by global-genome nucleotide excision repair accounts for the high mutagenicity and persistence of aristolactam-DNA adducts, *Nucleic Acids Res.* 40 (2012) 2494–2505. [PubMed: 22121226]
- [16]. Grollman AP, Shibutani S, Moriya M, Miller F, Wu L, Moll U, Suzuki N, Fernandes A, Rosenquist T, Medverec Z, Jakovina K, Brdar B, Slade N, Turesky RJ, Goodenough AK, Rieger R, Vukelic M, Jelakovic B, Aristolochic acid and the etiology of endemic (Balkan) nephropathy, *Proc. Natl. Acad. Sci. USA* 104 (2007) 12129–12134. [PubMed: 17620607]
- [17]. Hoang ML, Chen CH, Sidorenko VS, He J, Dickman KG, Yun BH, Moriya M, Niknafs N, Douville C, Karchin R, Turesky RJ, Pu YS, Vogelstein B, Papadopoulos N, Grollman AP, Kinzler

KW, Rosenquist TA, Mutational signature of aristolochic acid exposure as revealed by whole-exome sequencing, *Sci. Transl. Med* 5 (2013) 197ra102.

[18]. Geacintov NE, Broyde S, Buterin T, Naegeli H, Wu M, Yan S, Patel DJ, Thermodynamic and structural factors in the removal of bulky DNA adducts by the nucleotide excision repair machinery, *Biopolymers*, 65 (2002) 202–210. [PubMed: 12228925]

[19]. Puimalainen MR, Ruthemann P, Min JH, Naegeli H, Xeroderma pigmentosum group C sensor: unprecedented recognition strategy and tight spatiotemporal regulation, *Cell. Mol. Life Sci* 73 (2016) 547–566. [PubMed: 26521083]

[20]. Schärer OD, Nucleotide excision repair in eukaryotes, *Cold Spring Harbor Perspect. Biol* 5 (2013) a012609.

[21]. Sugawara K, Molecular mechanisms of DNA damage recognition for mammalian nucleotide excision repair, *DNA Repair*. 44 (2016) 110–117. [PubMed: 27264556]

[22]. Sugawara K, Ng JM, Masutani C, Iwai S, van der Spek PJ, Eker AP, Hanaoka F, Bootsma D, Hoeijmakers JH, Xeroderma pigmentosum group C protein complex is the initiator of global genome nucleotide excision repair, *Mol Cell*. 2 (1998) 223–232. [PubMed: 9734359]

[23]. Aboussekra A, Biggerstaff M, Shivji MK, Vilpo JA, Moncollin V, Podust VN, Protic M, Hubscher U, Egly JM, Wood RD, Mammalian DNA nucleotide excision repair reconstituted with purified protein components, *Cell*. 80 (1995) 859–868. [PubMed: 7697716]

[24]. Mu D, Park CH, Matsunaga T, Hsu DS, Reardon JT, Sancar A, Reconstitution of human DNA repair excision nuclease in a highly defined system, *J. Biol. Chem* 270 (1995) 2415–2418. [PubMed: 7852297]

[25]. Araujo SJ, Tirode F, Coin F, Pospiech H, Syvaaja JE, Stucki M, Hubscher U, Egly JM, Wood RD, Nucleotide excision repair of DNA with recombinant human proteins: definition of the minimal set of factors, active forms of TFIIH, and modulation by CAK, *Genes Dev*. 14 (2000) 349–359. [PubMed: 10673506]

[26]. Evans E, Fellows J, Coffer A, Wood RD, Open complex formation around a lesion during nucleotide excision repair provides a structure for cleavage by human XPG protein, *Embo J*. 16 (1997) 625–638. [PubMed: 9034344]

[27]. Riedl T, Hanaoka F, Egly JM, The comings and goings of nucleotide excision repair factors on damaged DNA, *Embo J*. 22 (2003) 5293–5303. [PubMed: 14517266]

[28]. Tapias A, Auriol J, Forget D, Enzlin JH, Schärer OD, Coin F, Coulombe B, Egly JM, Ordered conformational changes in damaged DNA induced by nucleotide excision repair factors, *J. Biol. Chem* 279 (2004) 19074–19083. [PubMed: 14981083]

[29]. Hoogstraten D, Bergink S, Ng JM, Verbiest VH, Luijsterburg MS, Geverts B, Raams A, Dinant C, Hoeijmakers JH, Vermeulen W, Houtsmuller AB, Versatile DNA damage detection by the global genome nucleotide excision repair protein XPC, *J. Cell Sci* 121 (2008) 2850–2859. [PubMed: 18682493]

[30]. Luijsterburg MS, von Bornstaedt G, Gourdin AM, Politi AZ, Mone MJ, Warmerdam DO, Goedhart J, Vermeulen W, van Driel R, Hofer T, Stochastic and reversible assembly of a multiprotein DNA repair complex ensures accurate target site recognition and efficient repair, *J. Cell Biol* 189 (2010) 445–463. [PubMed: 20439997]

[31]. Volker M, Mone MJ, Karmakar P, van Hoffen A, Schul W, Vermeulen W, Hoeijmakers JH, van Driel R, van Zeeland AA, Mullenders LH, Sequential assembly of the nucleotide excision repair factors in vivo, *Mol. Cell* 8 (2001) 213–224. [PubMed: 11511374]

[32]. Min JH, Pavletich NP, Recognition of DNA damage by the Rad4 nucleotide excision repair protein, *Nature*. 449 (2007) 570–575. [PubMed: 17882165]

[33]. Camenisch U, Trautlein D, Clement FC, Fei J, Leitenstorfer A, Ferrando-May E, Naegeli H, Two-stage dynamic DNA quality check by xeroderma pigmentosum group C protein, *EMBO J*. 28 (2009) 2387–2399. [PubMed: 19609301]

[34]. Buterin T, Meyer C, Giese B, Naegeli H, DNA quality control by conformational readout on the undamaged strand of the double helix, *Chem. Biol* 12 (2005) 913–922. [PubMed: 16125103]

[35]. Hess MT, Gunz D, Luneva N, Geacintov NE, Naegeli H, Base pair conformation-dependent excision of benzo[a]pyrene diol epoxide-guanine adducts by human nucleotide excision repair enzymes, *Mol. Cell. Biol* 17 (1997) 7069–7076. [PubMed: 9372938]

[36]. Hess MT, Schwitter U, Petretta M, Giese B, Naegeli H, Bipartite substrate discrimination by human nucleotide excision repair, *Proc. Natl. Acad. Sci. USA* 94 (1997) 6664–6669. [PubMed: 9192622]

[37]. Chen X, Velmurugu Y, Zheng G, Park B, Shim Y, Kim Y, Liu L, Van Houten B, He C, Ansari A, Min JH, Kinetic gating mechanism of DNA damage recognition by Rad4/XPC, *Nat. Commun* 6 (2015) 5849. [PubMed: 25562780]

[38]. Velmurugu Y, Chen X, Slogoff Sevilla P, Min JH, Ansari A, Twist-open mechanism of DNA damage recognition by the Rad4/XPC nucleotide excision repair complex, *Proc. Natl. Acad. Sci. USA* 113 (2016) E2296–2305. [PubMed: 27035942]

[39]. Kong M, Liu L, Chen X, Driscoll KI, Mao P, Bohm S, Kad NM, Watkins SC, Bernstein KA, Wyrick JJ, Min JH, Van Houten B, Single-Molecule Imaging Reveals that Rad4 Employs a Dynamic DNA Damage Recognition Process, *Mol. Cell* 64 (2016) 376–387. [PubMed: 27720644]

[40]. Sugasawa K, Akagi J, Nishi R, Iwai S, Hanaoka F, Two-step recognition of DNA damage for mammalian nucleotide excision repair: Directional binding of the XPC complex and DNA strand scanning, *Mol. Cell* 36 (2009) 642–653. [PubMed: 19941824]

[41]. Li CL, Golebiowski FM, Onishi Y, Samara NL, Sugasawa K, Yang W, Tripartite DNA Lesion Recognition and Verification by XPC, TFIIH, and XPA in Nucleotide Excision Repair, *Mol. Cell* 59 (2015) 1025–1034. [PubMed: 26384665]

[42]. Mu H, Geacintov NE, Zhang Y, Broyde S, Recognition of Damaged DNA for Nucleotide Excision Repair: A Correlated Motion Mechanism with a Mismatched cis-syn Thymine Dimer Lesion, *Biochemistry* 54 (2015) 5263–5267. [PubMed: 26270861]

[43]. Mu H, Geacintov NE, Min JH, Zhang Y, Broyde S, Nucleotide Excision Repair Lesion-Recognition Protein Rad4 Captures a Pre-Flipped Partner Base in a Benzo[a]pyrene-Derived DNA Lesion: How Structure Impacts the Binding Pathway, *Chem Res. Tox* 30 (2017) 1344–1354.

[44]. Geacintov NE, Cosman M, Hingerty BE, Amin S, Broyde S, Patel DJ, NMR solution structures of stereoisometric covalent polycyclic aromatic carcinogen-DNA adduct: principles, patterns, and diversity, *Chem Res. Tox* 10 (1997) 111–146.

[45]. Cai Y, Patel DJ, Broyde S, Geacintov NE, Base sequence context effects on nucleotide excision repair, *J. Nucleic Acids* 2010 (2010), 174252 [PubMed: 20871811]

[46]. Kropachev K, Kolbanovskii M, Cai Y, Rodriguez F, Kolbanovskii A, Liu Y, Zhang L, Amin S, Patel D, Broyde S, Geacintov NE, The sequence dependence of human nucleotide excision repair efficiencies of benzo[a]pyrene-derived DNA lesions: insights into the structural factors that favor dual incisions, *J. Mol. Biol* 386 (2009) 1193–1203. [PubMed: 19162041]

[47]. Mocquet V, Kropachev K, Kolbanovskiy M, Kolbanovskiy A, Tapias A, Cai Y, Broyde S, Geacintov NE, Egly JM, The human DNA repair factor XPC-HR23B distinguishes stereoisomeric benzo[a]pyrenyl-DNA lesions, *Embo J.* 26 (2007) 2923–2932. [PubMed: 17525733]

[48]. Cosman M, de los Santos C, Fiala R, Hingerty BE, Ibanez V, Luna E, Harvey R, Geacintov NE, Broyde S, Patel DJ, Solution conformation of the (+)-cis-anti-[BP]dG adduct in a DNA duplex: intercalation of the covalently attached benzo[a]pyrenyl ring into the helix and displacement of the modified deoxyguanosine, *Biochemistry* 32 (1993) 4145–4155. [PubMed: 8476845]

[49]. Reeves DA, Mu H, Kropachev K, Cai Y, Ding S, Kolbanovskiy A, Kolbanovskiy M, Chen Y, Krzeminski J, Amin S, Patel DJ, Broyde S, Geacintov NE, Resistance of bulky DNA lesions to nucleotide excision repair can result from extensive aromatic lesion-base stacking interactions, *Nucleic Acids Res.* 39 (2011) 8752–8764. [PubMed: 21764772]

[50]. Yeo JE, Khoo A, Fagbemi AF, Schärer OD, The efficiencies of damage recognition and excision correlate with duplex destabilization induced by acetylaminofluorene adducts in human nucleotide excision repair, *Chem Res. Tox* 25 (2012) 2462–2468.

[51]. Batty D, Rapic'-Otrin V, Levine AS, Wood RD, Stable Binding of Human XPC Complex to Irradiated DNA Confers Strong Discrimination for Damaged Sites, *J. Mol. Biol* 300 (2000) 275–290. [PubMed: 10873465]

[52]. Lee YC, Cai Y, Mu H, Broyde S, Amin S, Chen X, Min JH, Geacintov NE, The relationships between XPC binding to conformationally diverse DNA adducts and their excision by the human NER system: is there a correlation? *DNA Repair* 19 (2014) 55–63. [PubMed: 24784728]

[53]. Alekseev S, Coin F, Orchestral maneuvers at the damaged sites in nucleotide excision repair, *Cell. Mol. Life Sci* 72 (2015) 2177–2186. [PubMed: 25681868]

[54]. Nemzow L, Lubin A, Zhang L, Gong F, XPC: Going where no DNA damage sensor has gone before, *DNA Repair* 36 (2015) 19–27. [PubMed: 26422135]

[55]. Wittschieben BO, Iwai S, Wood RD, DDB1-DDB2 (xeroderma pigmentosum group E) protein complex recognizes a cyclobutane pyrimidine dimer, mismatches, apurinic/apyrimidinic sites, and compound lesions in DNA, *J. Biol. Chem* 280 (2005) 39982–39989. [PubMed: 16223728]

[56]. Chu G, Chang E, Xeroderma pigmentosum group E cells lack a nuclear factor that binds to damaged DNA, *Science* 242 (1988) 564–567. [PubMed: 3175673]

[57]. Fujiwara Y, Masutani C, Mizukoshi T, Kondo J, Hanaoka F, Iwai S, Characterization of DNA recognition by the human UV-damaged DNA-binding protein, *J. Biol. Chem* 274 (1999) 20027–20033. [PubMed: 10391953]

[58]. Fischer ES, Scrima A, Bohm K, Matsumoto S, Lingaraju GM, Fatty M, Yasuda T, Cavadini S, Wakasugi M, Hanaoka F, Iwai S, Gut H, Sugasawa K, Thoma NH, The molecular basis of CRL4DDB2/CSA ubiquitin ligase architecture, targeting, and activation, *Cell* 147 (2011) 1024–1039. [PubMed: 22118460]

[59]. Scrima A, Konickova R, Czyzewski BK, Kawasaki Y, Jeffrey PD, Groisman R, Nakatani Y, Iwai S, Pavletich NP, Thoma NH, Structural basis of UV DNA-damage recognition by the DDB1-DDB2 complex, *Cell* 135 (2008) 1213–1223. [PubMed: 19109893]

[60]. Yeh JI, Levine AS, Du S, Chinte U, Ghodke H, Wang H, Shi H, Hsieh CL, Conway JF, Van Houten B, Rapic-Otrin V, Damaged DNA induced UV-damaged DNA-binding protein (UV-DDB) dimerization and its roles in chromatinized DNA repair, *Proc. Natl. Acad. Sci. USA* 109 (2012) E2737–2746. [PubMed: 22822215]

[61]. Tang JY, Hwang BJ, Ford JM, Hanawalt PC, Chu G, Xeroderma pigmentosum p48 gene enhances global genomic repair and suppresses UV-induced mutagenesis, *Mol. Cell* 5 (2000) 737–744. [PubMed: 10882109]

[62]. Fitch ME, Nakajima S, Yasui A, Ford JM, In vivo recruitment of XPC to UV-induced cyclobutane pyrimidine dimers by the DDB2 gene product, *J. Biol. Chem* 278 (2003) 46906–46910. [PubMed: 12944386]

[63]. Groisman R, Polanowska J, Kuraoka I, Sawada J, Saijo M, Drapkin R, Kisselev AF, Tanaka K, Nakatani Y, The ubiquitin ligase activity in the DDB2 and CSA complexes is differentially regulated by the COP9 signalosome in response to DNA damage, *Cell* 113 (2003) 357–367. [PubMed: 12732143]

[64]. Sugasawa K, Okuda Y, Saijo M, Nishi R, Matsuda N, Chu G, Mori T, Iwai S, Tanaka K, Tanaka K, Hanaoka F, UV-induced ubiquitylation of XPC protein mediated by UV-DDB-ubiquitin ligase complex, *Cell* 121 (2005) 387–400. [PubMed: 15882621]

[65]. Puimalainen MR, Lessel D, Ruthemann P, Kaczmarek N, Bachmann K, Ramadan K, Naegeli H, Chromatin retention of DNA damage sensors DDB2 and XPC through loss of p97 segregase causes genotoxicity, *Nat. Commun* 5 (2014) 3695. [PubMed: 24770583]

[66]. Akita M, Tak YS, Shimura T, Matsumoto S, Okuda-Shimizu Y, Shimizu Y, Nishi R, Saitoh H, Iwai S, Mori T, Ikura T, Sakai W, Hanaoka F, Sugasawa K, SUMOylation of xeroderma pigmentosum group C protein regulates DNA damage recognition during nucleotide excision repair, *Sci. Rep* 5 (2015) 10984. [PubMed: 26042670]

[67]. van Cuijk L, van Belle GJ, Turkyilmaz Y, Poulsen SL, Janssens RC, Theil AF, Sabatella M, Lans H, Mailand N, Houtsmuller AB, Vermeulen W, Marteijn JA, SUMO and ubiquitin-dependent XPC exchange drives nucleotide excision repair, *Nat. Commun* 6 (2015) 7499. [PubMed: 26151477]

[68]. Smerdon MJ, Lieberman MW, Nucleosome rearrangement in human chromatin during UV-induced DNA- repair synthesis, *Proc. Natl. Acad. Sci. USA* 75 (1978) 4238–4241. [PubMed: 279912]

[69]. Stadler J, Richly H, Regulation of DNA Repair Mechanisms: How the Chromatin Environment Regulates the DNA Damage Response, *Int. J. Mol. Sci.* 18 (2017).

[70]. Polo SE, Almouzni G, Chromatin dynamics after DNA damage: The legacy of the access-repair-restore model, *DNA Repair* 36 (2015) 114–121. [PubMed: 26429064]

[71]. Balbo Pogliano C, Gatti M, Ruthemann P, Garajova Z, Penengo L, Naegeli H, ASH1L histone methyltransferase regulates the handoff between damage recognition factors in global-genome nucleotide excision repair, *Nat. Commun* 8 (2017) 1333. [PubMed: 29109511]

[72]. Ruthemann P, Balbo Pogliano C, Codilupi T, Garajova Z, Naegeli H, Chromatin remodeler CHD1 promotes XPC-to-TFIID handover of nucleosomal UV lesions in nucleotide excision repair, *EMBO J.* 36 (2017) 3372–3386. [PubMed: 29018037]

[73]. Kakumu E, Nakanishi S, Shiratori HM, Kato A, Kobayashi W, Machida S, Yasuda T, Adachi N, Saito N, Ikura T, Kurumizaka H, Kimura H, Yokoi M, Sakai W, Sugawara K, Xeroderma pigmentosum group C protein interacts with histones: regulation by acetylated states of histone H3, *Genes Cells* 22 (2017) 310–327. [PubMed: 28233440]

[74]. Luijsterburg MS, Lindh M, Acs K, Vrouwe MG, Pines A, van Attikum H, Mullenders LH, Dantuma NP, DDB2 promotes chromatin decondensation at UV-induced DNA damage, *J. Cell Biol.* 197 (2012) 267–281. [PubMed: 22492724]

[75]. Maltseva EA, Rechkunova NI, Sukhanova MV, Lavrik OI, Poly(ADP-ribose) Polymerase 1 Modulates Interaction of the Nucleotide Excision Repair Factor XPC-RAD23B with DNA via Poly(ADP-ribosylation), *J. Biol. Chem.* 290 (2015) 21811–21820. [PubMed: 26170451]

[76]. Pines A, Vrouwe MG, Marteijn JA, Typas D, Luijsterburg MS, Cansoy M, Hensbergen P, Deelder A, de Groot A, Matsumoto S, Sugawara K, Thoma N, Vermeulen W, Vrieling H, Mullenders L, PARP1 promotes nucleotide excision repair through DDB2 stabilization and recruitment of ALC1, *J. Cell Biol.* 199 (2012) 235–249. [PubMed: 23045548]

[77]. Robu M, Shah RG, Petitclerc N, Brind’Amour J, Kandan-Kulangara F, Shah GM, Role of poly(ADP-ribose) polymerase-1 in the removal of UV-induced DNA lesions by nucleotide excision repair, *Proc. Natl. Acad. Sci. USA* 110 (2013) 1658–1663. [PubMed: 23319653]

[78]. Robu M, Shah RG, Purohit NK, Zhou P, Naegeli H, Shah GM, Poly(ADP-ribose) polymerase 1 escorts XPC to UV-induced DNA lesions during nucleotide excision repair, *Proc. Natl. Acad. Sci. USA* 114 (2017) E6847–E6856. [PubMed: 28760956]

[79]. Compe E, Egly JM, Nucleotide Excision Repair and Transcriptional Regulation: TFIID and Beyond, *Annu. Rev. Biochem.* 85 (2016) 265–290. [PubMed: 27294439]

[80]. Coin F, Okseny V, Mocquet V, Groh S, Blattner C, Egly JM, Nucleotide excision repair driven by the dissociation of CAK from TFIID, *Mol. Cell* 31 (2008) 9–20. [PubMed: 18614043]

[81]. Kemp MG, Reardon JT, Lindsey-Boltz LA, Sancar A, Mechanism of release and fate of excised oligonucleotides during nucleotide excision repair, *J. Biol. Chem.* 287 (2012) 22889–22899. [PubMed: 22573372]

[82]. Hu J, Choi JH, Gaddameedhi S, Kemp MG, Reardon JT, Sancar A, Nucleotide excision repair in human cells: fate of the excised oligonucleotide carrying DNA damage in vivo, *J. Biol. Chem.* 288 (2013) 20918–20926. [PubMed: 23749995]

[83]. Fan L, DuPrez KT, XPD: An unconventional SF2 DNA helicase, *Prog. Biophys. Mol. Biol.* 117 (2015) 174–181. [PubMed: 25641424]

[84]. Okseny V, de Jesus BB, Zhovmer A, Egly JM, Coin F, Molecular insights into the recruitment of TFIID to sites of DNA damage, *EMBO J.*, 28 (2009) 2971–2980. [PubMed: 19713942]

[85]. Kuper J, Braun C, Elias A, Michels G, Sauer F, Schmitt DR, Poterszman A, Egly JM, Kisker C, In TFIID, XPD helicase is exclusively devoted to DNA repair, *PLoS Biol.* 12 (2014) e1001954. [PubMed: 25268380]

[86]. Winkler GS, Araujo SJ, Fiedler U, Vermeulen W, Coin F, Egly JM, Hoeijmakers JH, Wood RD, Timmers HT, Weeda G, TFIID with inactive XPD helicase functions in transcription initiation but is defective in DNA repair, *J. Biol. Chem.* 275 (2000) 4258–4266. [PubMed: 10660593]

[87]. Fan L, Fuss JO, Cheng QJ, Arvai AS, Hammel M, Roberts VA, Cooper PK, Tainer JA, XPD helicase structures and activities: insights into the cancer and aging phenotypes from XPD mutations, *Cell* 133 (2008) 789–800. [PubMed: 18510924]

[88]. Liu H, Rudolf J, Johnson KA, McMahon SA, Oke M, Carter L, McRobbie AM, Brown SE, Naismith JH, White MF, Structure of the DNA repair helicase XPD, *Cell* 133 (2008) 801–812. [PubMed: 18510925]

[89]. Wolski SC, Kuper J, Hanzelmann P, Truglio JJ, Croteau DL, Van Houten B, Kisker C, Crystal structure of the FeS cluster-containing nucleotide excision repair helicase XPD, *PLoS Biol.* 6 (2008) e149. [PubMed: 18578568]

[90]. Mathieu N, Kaczmarek N, Naegeli H, Strand- and site-specific DNA lesion demarcation by the xeroderma pigmentosum group D helicase, *Proc. Natl. Acad. Sci. USA* 107 (2010) 17545–17550. [PubMed: 20876134]

[91]. Kuper J, Wolski SC, Michels G, Kisker C, Functional and structural studies of the nucleotide excision repair helicase XPD suggest a polarity for DNA translocation, *EMBO J.* 31 (2012) 494–502. [PubMed: 22081108]

[92]. Pugh RA, Wu CG, Spies M, Regulation of translocation polarity by helicase domain 1 in SF2B helicases, *EMBO J.* 31 (2012) 503–514. [PubMed: 22081110]

[93]. Naegeli H, Bardwell L, Friedberg EC, The DNA helicase and adenosine triphosphatase activities of yeast Rad3 protein are inhibited by DNA damage. A potential mechanism for damage-specific recognition, *J. Biol. Chem.* 267 (1992) 392–398. [PubMed: 1309743]

[94]. Mathieu N, Kaczmarek N, Ruthemann P, Luch A, Naegeli H, DNA quality control by a lesion sensor pocket of the xeroderma pigmentosum group D helicase subunit of TFIIH, *Curr. Biol.* 23 (2013) 204–212. [PubMed: 23352696]

[95]. Wirth N, Gross J, Roth HM, Buechner CN, Kisker C, Tessmer I, Conservation J Biol. Chem 291 (2016) 18932–18946.

[96]. Constantinescu-Aruxandei D, Petrovic-Stojanovska B, Penedo JC, White MF, Naismith JH, Mechanism of DNA loading by the DNA repair helicase XPD, *Nucleic Acids Res.* 44 (2016) 2806–2815. [PubMed: 26896802]

[97]. Camenisch U, Dip R, Schumacher SB, Schuler B, Naegeli H, Recognition of helical kinks by xeroderma pigmentosum group A protein triggers DNA excision repair, *Nat. Struct. Mol. Biol.* 13 (2006) 278–284. [PubMed: 16491090]

[98]. Missura M, Buterin T, Hindges R, Hubscher U, Kasparkova J, Brabec V, Naegeli H, Double-check probing of DNA bending and unwinding by XPA-RPA: an architectural function in DNA repair, *Embo J.* 20 (2001) 3554–3564. [PubMed: 11432842]

[99]. Lafrance-Vanasse J, Arseneault G, Cappadocia L, Legault P, Omichinski JG, Structural and functional evidence that Rad4 competes with Rad2 for binding to the Tfb1 subunit of TFIIH in NER, *Nucleic Acids Res.* 41 (2013) 2736–2745. [PubMed: 23295669]

[100]. Okuda M, Kinoshita M, Kakumu E, Sugasawa K, Nishimura Y, Structural Insight into the Mechanism of TFIIH Recognition by the Acidic String of the Nucleotide Excision Repair Factor XPC, *Structure* 23 (2015) 1821–1831.

[101]. de Jesus B.M. Bernardes, Bjørås M, Coin F, Egly JM, Dissection of the molecular defects caused by pathogenic mutations in the DNA repair factor XPC, *Mol. Cell. Biol.* 28 (2008) 1225–1235.

[102]. Uchida A, Sugasawa K, Masutani C, Dohmae N, Araki M, Yokoi M, Ohkuma Y, Hanaoka F, The carboxy-terminal domain of the XPC protein plays a crucial role in nucleotide excision repair through interactions with transcription factor IIH, *DNA Repair.* 1 (2002) 449–461. [PubMed: 12509233]

[103]. Yokoi M, Masutani C, Maekawa T, Sugasawa K, Ohkuma Y, Hanaoka F, The xeroderma pigmentosum group C protein complex XPC-HR23B plays an important role in the recruitment of transcription factor IIH to damaged DNA, *J. Biol. Chem.* 215 (2000) 9810–9815.

[104]. Greber BJ, Nguyen THD, Fang J, Afonine PV, Adams PD, Nogales E, The cryo-electron microscopy structure of human transcription factor IIH, *Nature* 549 (2017) 414–417. [PubMed: 28902838]

[105]. Schilbach S, Hantsche M, Tegunov D, Dienemann C, Wigge C, Urlaub H, Cramer P, Structures of transcription pre-initiation complex with TFIIH and Mediator, *Nature* 551 (2017) 204–209. [PubMed: 29088706]

[106]. Sugitani N, Sivley RM, Perry KE, Capra JA, Chazin WJ, XPA: A key scaffold for human nucleotide excision repair, *DNA Repair* 44 (2016) 123–135. [PubMed: 27247238]

[107]. Tsodikov OV, Ivanov D, Orelli B, Staresinic L, Shoshani I, Oberman R, Schärer OD, Wagner G, Ellenberger T, Structural basis for the recruitment of ERCC1-XPF to nucleotide excision repair complexes by XPA, *EMBO J.* 26 (2007) 4768–4776. [PubMed: 17948053]

[108]. Sijbers AM, de Laat WL, Ariza RR, Biggerstaff M, Wei YF, Moggs JG, Carter KC, Shell BK, Evans E, de Jong MC, Rademakers S, de Rooij J, Jaspers NG, Hoeijmakers JH, Wood RD, Xeroderma pigmentosum group F caused by a defect in a structure- specific DNA repair endonuclease, *Cell* 86 (1996) 811–822. [PubMed: 8797827]

[109]. Araujo SJ, Nigg EA, Wood RD, Strong functional interactions of TFIIH with XPC and XPG in human DNA nucleotide excision repair, without a preassembled repairosome, *Mol. Cell. Biol* 21 (2001) 2281–2291. [PubMed: 11259578]

[110]. Ito S, Kuraoka I, Chymkowitch P, Compe E, Takedachi A, Ishigami C, Coin F, Egly JM, Tanaka K, XPG Stabilizes TFIIH, Allowing Transactivation of Nuclear Receptors: Implications for Cockayne Syndrome in XP-G/CS Patients, *Mol. Cell* 26 (2007) 231–243. [PubMed: 17466625]

[111]. Moser J, Kool H, Giakzidis I, Caldecott K, Mullenders LH, Fousteri MI, Sealing of chromosomal DNA nicks during nucleotide excision repair requires XRCC1 and DNA ligase III alpha in a cell-cycle-specific manner, *Mol. Cell* 27 (2007) 311–323. [PubMed: 17643379]

[112]. Ogi T, Limsirichaikul S, Overmeer RM, Volker M, Takenaka K, Cloney R, Nakazawa Y, Niimi A, Miki Y, Jaspers NG, Mullenders LH, Yamashita S, Fousteri MI, Lehmann AR, Three DNA polymerases, recruited by different mechanisms, carry out NER repair synthesis in human cells, *Mol. Cell* 37 (2010) 714–727. [PubMed: 20227374]

[113]. Staresinic L, Fagbemi AF, Enzlin JH, Gourdin AM, Wijgers N, Dunand-Sauthier I, Giglia-Mari G, Clarkson SG, Vermeulen W, Schärer OD, Coordination of dual incision and repair synthesis in human nucleotide excision repair, *EMBO J.* 28 (2009) 1111–1120. [PubMed: 19279666]

[114]. Case DA, Cheatham TE, 3rd, Darden T, Gohlke H, Luo R, Merz KM, Jr., Onufriev A, Simmerling C, Wang B, Woods RJ, The Amber biomolecular simulation programs, *J. Comput. Chem* 26 (2005) 1668–1688. [PubMed: 16200636]

[115]. Rooklin D, Wang C, Katigbak J, Arora PS, Zhang Y, AlphaSpace: Fragment-Centric Topographical Mapping To Target Protein-Protein Interaction Interfaces, *J. Chem. Inf. Model* 55 (2015) 1585–1599. [PubMed: 26225450]

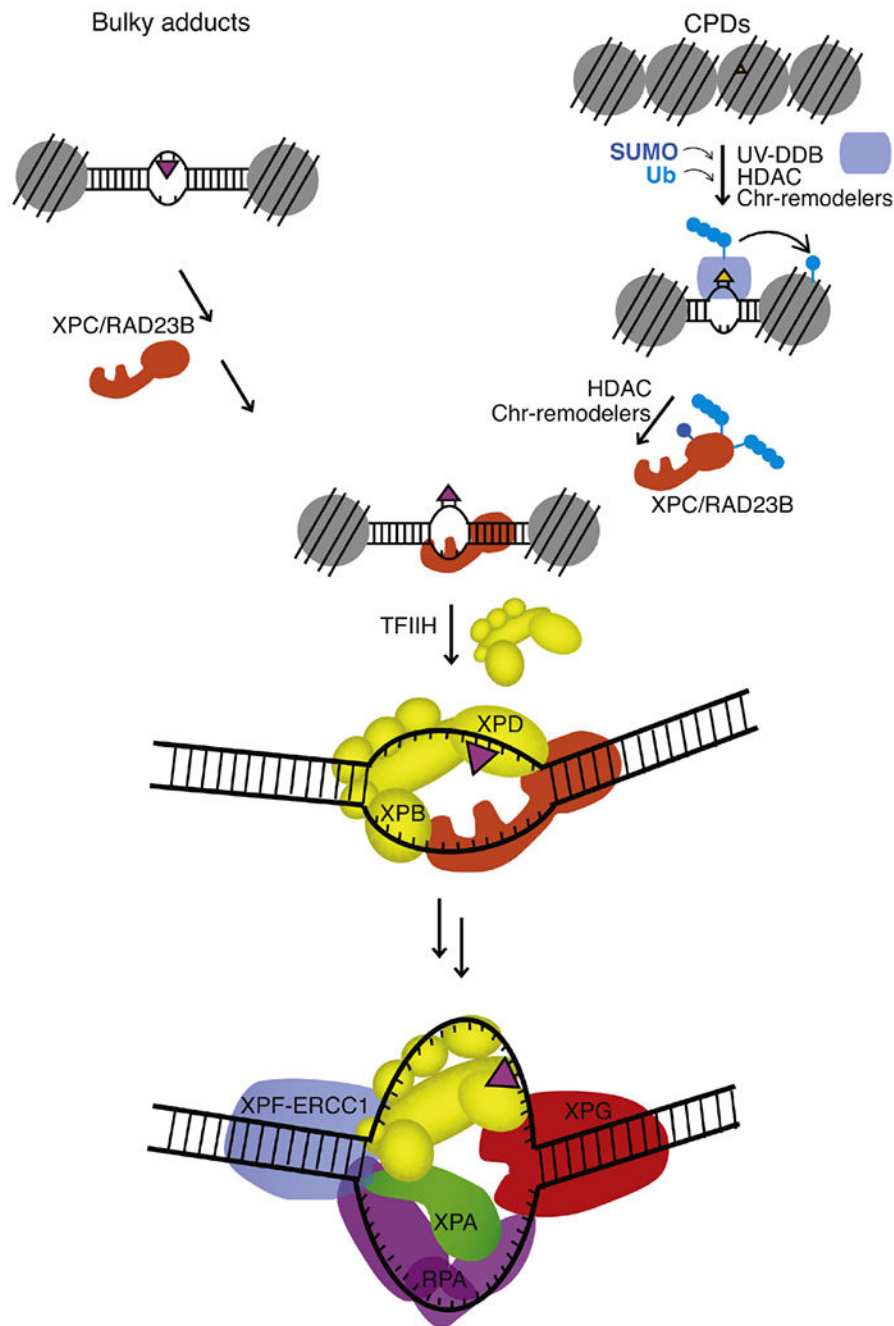


Fig. 1. Model of the mechanisms of damage recognition in NER.

Distorting bulky DNA lesions are directly recognized by XPC-RAD23B. Less distorting lesions in chromatin, especially CPDs, are first detected by UV-DDB. Chromatin structure is altered with a series of modifications by ubiquitin and sumo as well as by the activities of histone modifiers and chromatin remodelers allowing XPC-RAD23B to gain access to the lesion. XPC-RAD23B recognizes the local helical destabilization caused by a DNA lesion and interacts with TFIIH, which loads on DNA near the lesion via its XPB subunit, allowing the helicase XPD to track along the DNA to verify the presence of the lesion. The inherent

asymmetry of the XPC-TFIIH-Lesion complex ensures proper loading of the pre-incision complex consisting of TFIIH, XPA, RPA, XPG and ERCC1-XPF to make a dual incision on the damaged strand to remove the damage as part of an oligonucleotide.

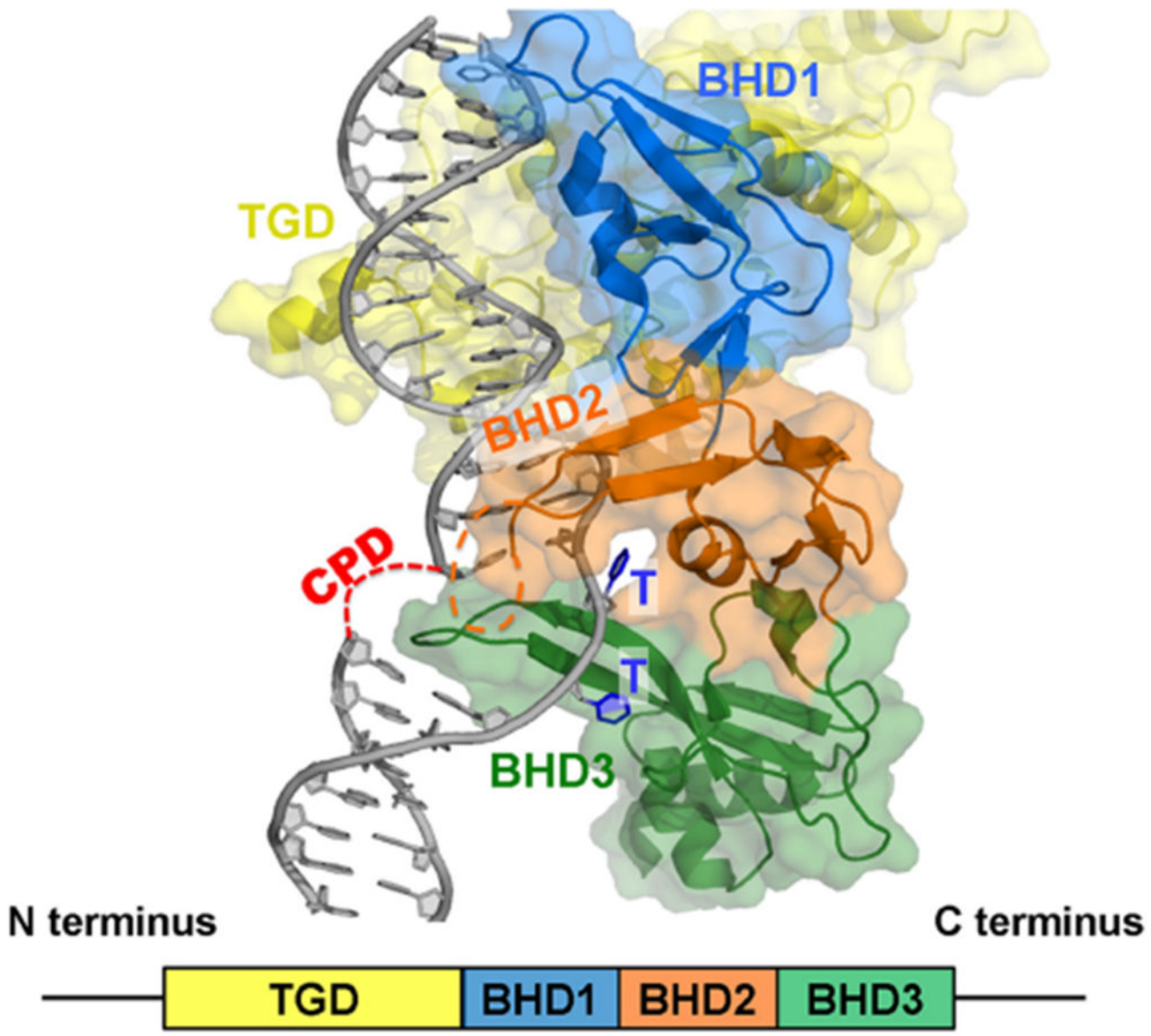


Fig. 2. Crystal structure of Rad4.

Rad4, the yeast orthologue of human XPC, productively bound to the CPD damaged DNA with mismatched thymines opposite the CPD (PDB ID: 2QSG [32]). The unresolved CPD (red) and BHD2 (orange) hairpin tip are indicated by dashed lines. The mismatched thymines (T) that are flipped into their binding pockets are indicated in blue. Color codes of other domains: TGD, yellow; BHD1, marine; BHD2, orange; BHD3, green; DNA, grey.

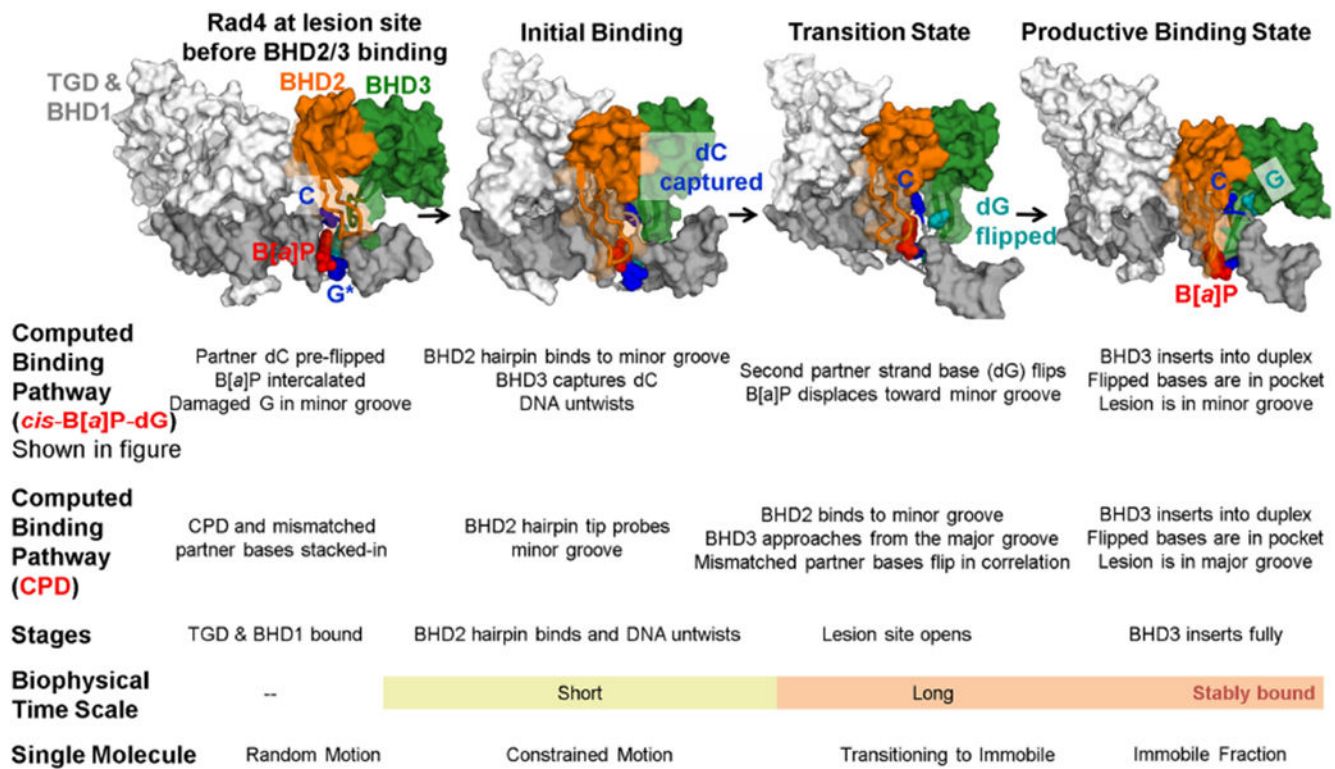


Fig. 3. Key binding states in the full pathway from initial to productive binding of Rad4. Structures represent Rad4 binding to a (+) *cis*-B[a]P-dG containing DNA duplex with extruded normal partner C obtained from molecular dynamics/free energy calculations [43]. The table also presents details concerning pathway simulations for the CPD lesion [42], which manifests key difference from the (+) *cis*-B[a]P-dG case. Insights from biophysical measurements are also summarized [37–39]. Color scheme as in Figure 2.

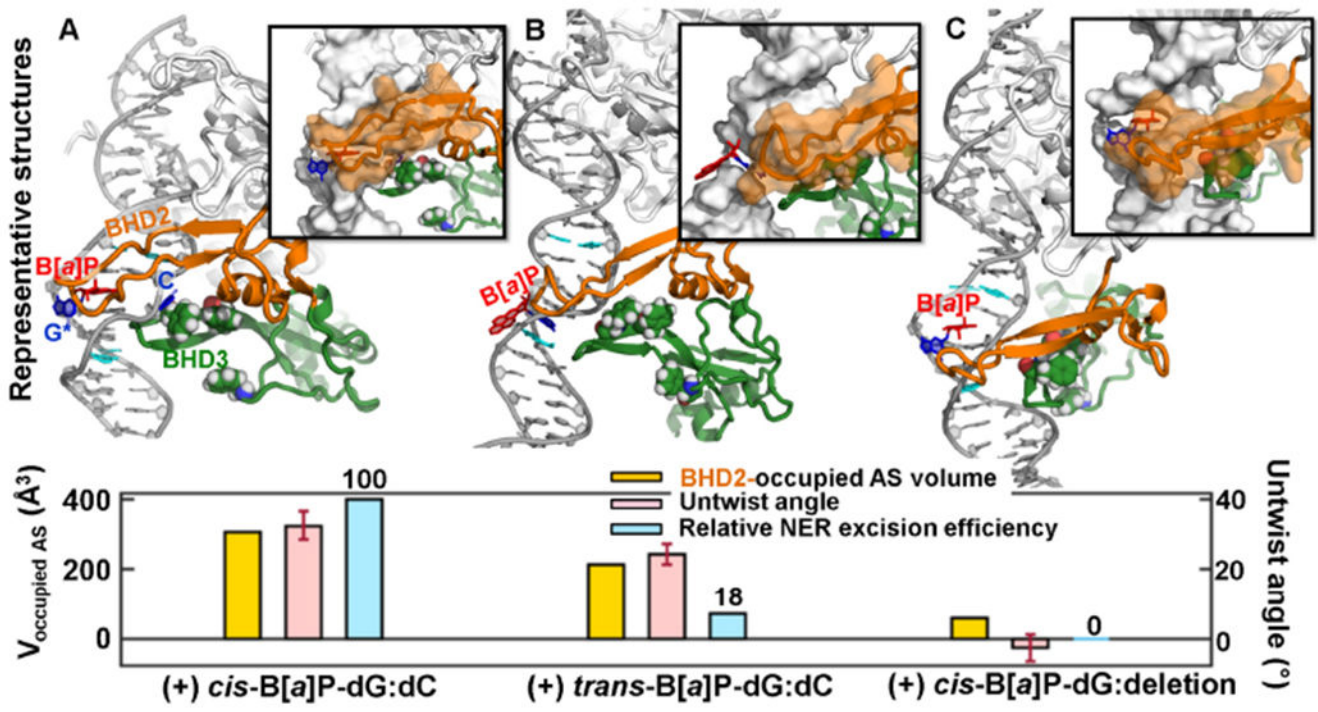


Fig. 4. Correlation of Rad4 BHD2 occupied alpha space volume, DNA untwist angle, and NER efficiency.

Representative structures, alpha space volumes occupied by BHD2 in the minor groove, and untwist angles obtained from MD simulations of Rad4 initial binding complexes, and experimental relative NER excision efficiencies [12] for the (+) *cis*-B[a]P-dG:dC, (+) *trans*-B[a]P-dG:dC and (+) *cis*-B[a]P-dG:deletion duplexes. Shown are the best representative structures of the trajectory from 1 - 1.5 μ s obtained using the AMBER 16 package [114]. Full size and zoomed in views are given for each structure. Occupied alpha-space volumes were calculated for the representative structures using AlphaSpace [115]. These volumes reflect the curvature and surface area of the DNA minor groove that is bound by BHD2. Each untwist angle is the difference between the twist angle over 5 base pair steps (between the cyan base pairs) before BHD2 enters the minor groove and after BHD2 has stably bound the minor groove and a stable twist angle has been achieved. This value reflects the untwisting induced by BHD2 binding to the minor groove around the lesion site.

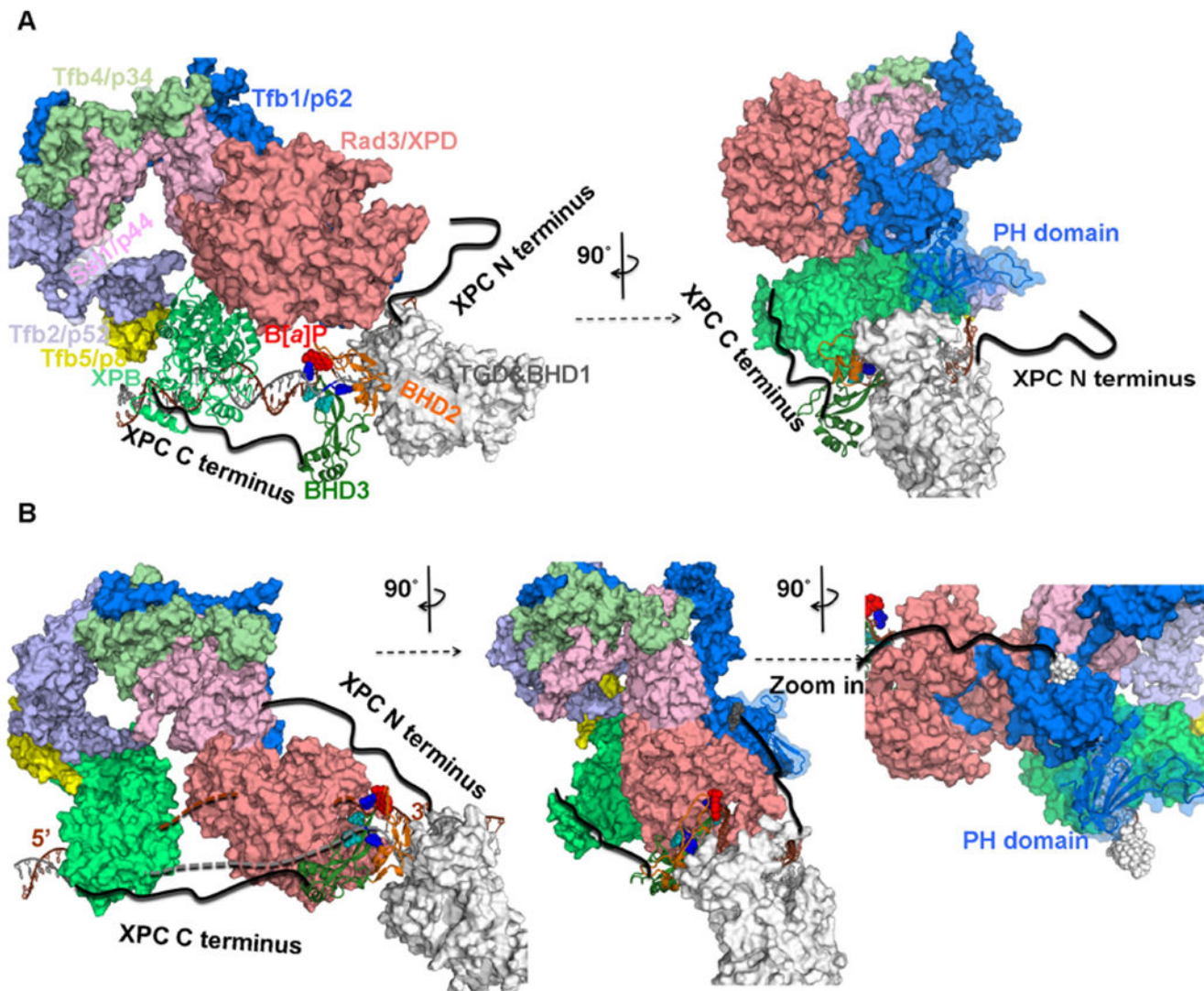


Figure 5. Structural Model for the Interplay of XPC and TFIIH.

A. Initial TFIIH binding mediated by the interaction of XPB with DNA and the N-terminus of XPC. **B.** Damage verification complex formation after XPD engages with the lesion and the N-terminus XPC binds to the PH domain of p62. The TFIIH complex was modeled based on the Cryo-EM structure of yeast TFIIH by Schilbach et al. (PDB ID: 5OQJ); in order to reveal more of the structure of the XPB N terminus, Ssl2/yeast XPB was replaced by the XPB structure in the Cryo-EM structure of human TFIIH by Greber et al. (PDB ID: 5OQF), through superposition of XPB residues 368-381 and 631-642 to Ssl2 residues 414-427 and 678-689. The undamaged DNA bound to XPB was modeled using DNA in PDB ID: 5OQJ. The lesion-containing DNA in complex with XPC was then modeled using the productively bound state of Rad4/XPC in complex with a *cis*-B[a]P-dG containing DNA [43]. For the XPC N terminal binding to the PH domain of Tfb1/yeast p62, we docked a section of the XPC N terminus (residues 109-156) to the PH domain, through superposition of the p62 PH domain from the solution structure of the complex between the XPC N terminus and the p62

PH domain (PDB ID: 2RVB) [100] to the PH domain in our TFIIH model. This section of the XPC N terminus is shown in gray spheres. In order to reveal the XPC N terminal binding to p62, the p62 is shown as a transparent surface in B.

Author Manuscript

Author Manuscript

Author Manuscript

Author Manuscript